Electronic Supplementary Material (ESI) for Metallomics

Quantification of Copper Binding to Amyloid Precursor Protein Domain 2 and its *Caenorhabditis elegans* Ortholog. Implications for Biological Function.

Su Ling Leong[1,2], Tessa R. Young[1,3], Kevin J. Barnham[1,4,5], Anthony G. Wedd[1,3], Mark G. Hinds*[,1,3], Zhiguang Xiao*[,1,3], Roberto Cappai*[,1,2]

From [1]Bio21 Molecular Science and Biotechnology Institute, [2]Department of Pathology, [3]School of Chemistry, [4]Department of Pharmacology, The University of Melbourne, Victoria 3010, Australia and [5]Florey Institute for Neuroscience and Mental Health, Victoria, Australia

Emails: mhinds@unimelb.edu.au; z.xiao@unimelb.edu.au; r.cappai@unimelb.edu.au

Supplementary Information

Analysis of Cu(II) binding to APP-D2 and APL1-D2

By direct metal ion titration: Titration of Cu(II) into a solution of APP-D2 (20 μM) in Mops buffer quenched the fluorescence intensity progressively until ca. two equiv of Cu(II) were added but with no clear turning point (Figure 3b, filled circles). The equivalent titration for a more concentrated solution (200 μM) generated a similar titration curve whose turning point was only marginally better defined (Figure 3b, empty triangles). These observations indicate that, when $[P]_{tot} \geq 20$ μM, the fraction of Cu(II) bound to protein P (i.e., $[Cu^{II}\text{-}P]/[Cu(II)]_{tot}$ in eqn 2) before the turning point was not sensitive to the free protein concentration [P] and thus the condition $K_D(1 + K_A[L]) << [P]$ must be met to allow $[Cu^{II}\text{-}P]/[Cu(II)]_{tot} \sim 1.0$. Consequently, when $[P]_{tot} \geq 20$ μM, eqn 1 is highly favoured toward forward direction, i.e., added Cu^{2+} ions are bound largely by the protein ligand P with little contribution from potential competing complexes 'Cu^{II}-L' until the Cu(II) binding site(s) were saturated after the apparent turning point at $[Cu]_{tot}/[P]_{tot} = 2.0$. Consequently, it can be concluded provisionally that APP-D2 can bind two equiv of Cu(II) at two separated sites, but that it is difficult to distinguish the binding affinities of these two putative sites at $[P]_{tot} \geq 20$ μM.

When the titration was conducted at a lower APP-D2 concentration (2.0 μM), the fluorescence quenching extended to ~ 5 equiv of Cu(II) (Figure 3b, filled triangles). At [Cu(II)]/[P] = 2.0, the quenching was only ~ 50% complete, suggesting that only about half of the Cu(II) sites in the protein were occupied. This indicates that eqn 1 is in effective equilibrium at total protein concentrations in the micromolar region. Then, from eqn 2, $K_D(1 + K_A[L]) \sim [P] \sim 1.0$ μM. Assuming that Cu_{aq}^{2+} is the only 'free' Cu(II) species present (eqn 1), then $K_A = 0$ and the affinity of the protein for Cu(II) can be expressed as $K_D \sim 1.0$ μM. However, this is unlikely, considering the high relative concentration of buffer Mops and other possible minor but

unknown Cu(II) ligands in the solution. Consequently, ['Cu^{II}-L'] > 0 (eqn 1), $K_A > 0$ and $K_D = (1 + K_A[L])^{-1}$ μM < 1.0 μM. Notably, the decline of the titration curves in Figure 3b was essentially linear, indicating that the Cu(II) affinities of the two possible sites in APP-D2 are comparable. These conclusions are supported by more quantitative experiments with $Cu^{II}(Gly)_2$ as a Cu^{2+} buffer (see below).

Equivalent titrations of Cu^{2+} into APL1-D2 solutions of respective concentrations 2.0 μM and 20 μM generated comparable titration curves to those of APP-D2 (Figure 3c). However, closer examination suggested that at least one of the two putative Cu(II) sites in APL1-D2 was somewhat weaker. In particular, Cu^{2+} titration of the diluted APL1-D2 solution at 2.0 μM shifted λ_{max} from 340 nm to 324 nm, likely due to sequential weak Cu(II) binding to different sites and the two fluorescence probes (Trp and Tyr) in APL1-D2 responding differentially (Figure S4). Assuming that one binding site is the N-terminus with comparable affinity to the equivalent site in APP-D2, the other weaker 'site' must be adventitious in nature. A comparison of primary sequence and 3D structure indicates absence of the second Cu(II) site in APL1-D2 (Figures 1, 2).

By competition for Cu(II) with Gly: Addition of increasing amounts of Gly into a series of solutions containing equal concentrations of Cu_2P (20 μM; P = APL1-D2 or APP-D2) recovered the protein fluorescence intensity partially (Figure 4a), demonstrating that eqn 3 was in equilibrium under the conditions and, consequently, that free [Cu^{2+}] may be calculated from eqn 5 at various titration points. The experiments were not able to distinguish the difference in Cu(II) affinities of the two sites in the proteins (Figure 4b). Assuming that they are comparable, then their K_D may be approximated by the free [Cu^{2+}] calculated at $\Delta F/\Delta F_{max} = 0.5$, i.e., at the titration point of $[Gly]_{tot}$ = 100 μM for P = APL1-D2 and 250 μM for P = APP-D2 where the free [Gly] concentrations were calculated to be 65 and 212 μM, respectively (Figure 4b; see

Figure S5 and the associated supporting information for the calculation). The weak buffer complex 'Cu^{II}-L' would be suppressed considerably by the added Gly ligand, i.e., $[Cu(II)]_{tot}$ – ['Cu^{II}-L'] – [Cu^{II}-P] ≈ $[Cu(II)]_{tot}$ – [Cu^{II}-P] and therefore an average Cu(II) K_D value was estimated from eqn 5 to be $10^{-6.8}$ and $10^{-7.8}$ M for APL1-D2 and APP-D2, respectively. These estimations were consistent with the estimation of $K_D < 10^{-6}$ M from direct metal ion titration in Figure 3. These affinities are weak, but the affinity for APP-D2 estimated in this work is about three orders of magnitude stronger than a previous estimation of $K_D \sim 10$ μM.[1]

By competition for Cu(II) with Aβ peptides: Titration of APP-D2 (20 μM) with Cu^{2+} in Mops buffer (50 mM, pH 7.3) quenched fluorescence intensity at 330 nm and generated titration curve (i) with an apparent turning point at Cu(II):APP-D2 ~ 2 (Figure 5b). An equivalent titration of a solution containing both APP-D2 (20 μM) and EDTA (40 μM) generated titration curve (iii). The turning point at Cu(II):APP-D2 = 2 is consistent with strong ligand EDTA ($K_D = 10^{-15.8}$ M at pH 7.3) sequestering the first two equiv of added Cu(II) and APP-D2 (with its two weaker binding sites) binding the metal ion once EDTA was exhausted.

The Cu(II) affinity of the Aβ16 peptide is set at a current consensus value of $K_D \sim 10^{-10}$ M at pH 7.4 for the site of highest affinity.[2-4] The peptide exhibits a second weaker site of affinity $K_D \sim 10^{-8.0}$ M.[4] Titration of a solution of APP-D2 (20 μM) and Aβ16 (40 μM) generated titration curve (iv). It is apparent that neither Cu(II) site in APP-D2 can compete with the site of highest affinity on Aβ16 (turning point at Cu(II):APP-D2 = 2) but that competition between APP-D2 and the weaker site on Aβ16 occurs after that.

Ac-Aβ16 features an N-terminus that is blocked by acetylation. This imposes a weaker affinity for Cu(II) ($K_D \sim 10^{-8}$ M).[5] Replacement of Aβ16 with Ac-Aβ16 provided titration (ii) in

which APP-D2 and Ac-Aβ16 compete for Cu(II) effectively. It is apparent that they have similar affinities for this metal ion.

References

1 L. Hesse, D. Beher, C. L. Masters and G. Multhaup, The beta A4 amyloid precursor protein binding to copper, *FEBS Lett* 1994, **349**, 109-116.

2 C. J. Sarell, C. D. Syme, S. E. Rigby and J. H. Viles, Copper(II) binding to amyloid-beta fibrils of Alzheimer's disease reveals a picomolar affinity: stoichiometry and coordination geometry are independent of Abeta oligomeric form, *Biochemistry* 2009, **48**, 4388-4402.

3 C. Sacco, R. A. Skowronsky, S. Gade, J. M. Kenney and A. M. Spuches, Calorimetric investigation of copper(II) binding to Abeta peptides: thermodynamics of coordination plasticity, *J. Biol. Inorg. Chem.* 2012, **17**, 531-541.

4 B. Alies, E. Renaglia, M. Rozga, W. Bal, P. Faller and C. Hureau, Cu(II) Affinity for the Alzheimer's Peptide: Tyrosine Fluorescence Studies Revisited, *Anal. Chem.* 2013, **85**, 1501-1508.

5 T. R. Young, A. G. Wedd and Z. Xiao, Unpublished observations.

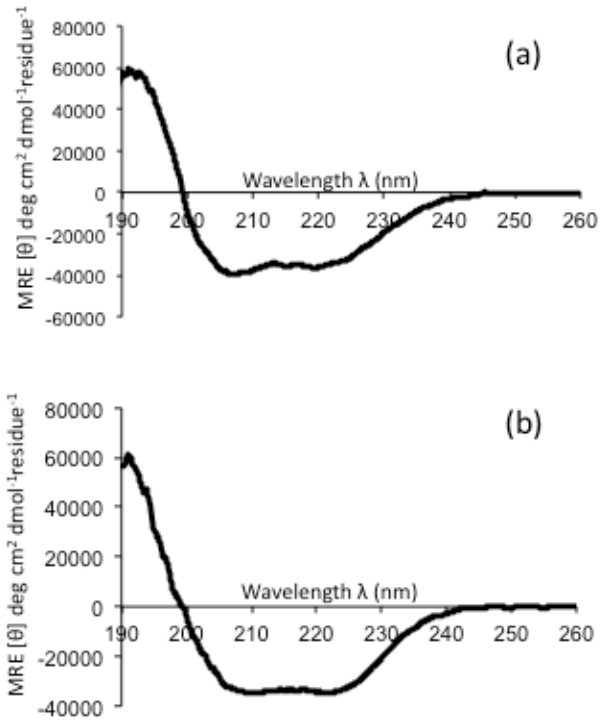

Figure S1. CD spectra in KPi buffer (10 mM, pH 7.0): (a) APL1-D2; (b) APP-D2.

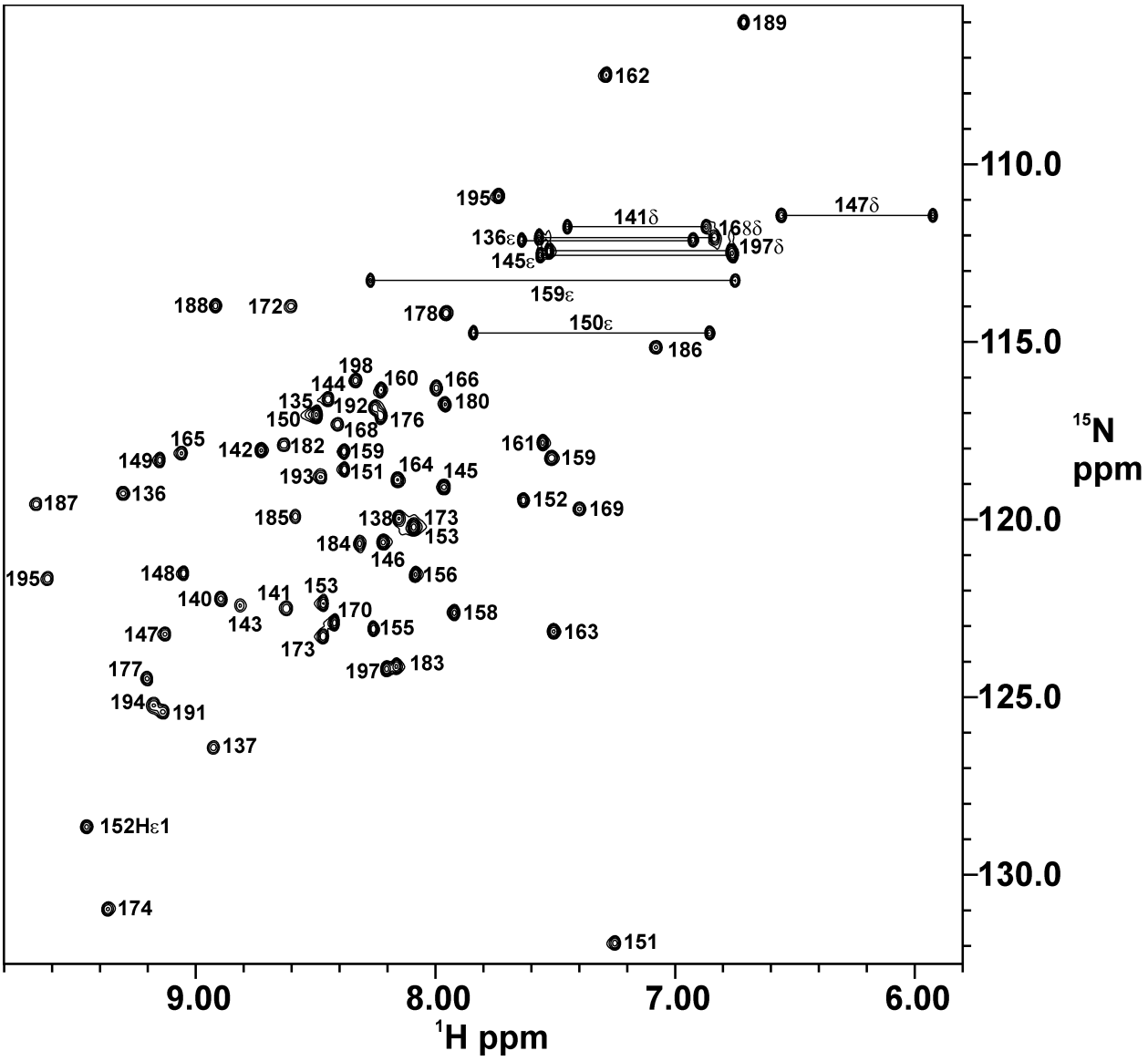

Figure S2. 800 MHz ^{1}H,^{15}N HSQC of *C. elegans* APL1-D2. Cross peaks are labelled with their sequence positions. Side chain amide resonances for Asn and Gln are connected with a bar. Details of the sample are given in the main text.

```
|Q10651_CAEEL HDCQFSHVNSRDQCNDYQHWKDEAGKQCKTKKSKGNKDMIVRSFAVLEPCALDMFTGVEFVCCPNDQTNKTDVQKTKEDE 212
|E3LE65_CAERE HDCQFSHVNSRDQCNDYQHWKDEAGKQCATKKSKDSKAMIVRSFAVLEPCALDMFTGVEFVCCPNDQTNKTSGHKADED- 211
|A8XKA6_CAEBR HDCQFSHVNSRDQCNDYQHWKDEAGKQCSGKKAKDTKSMIVRSFAVLEPCALDMFTGVEFVCCPNDQTNKTTT----EDE 208
|G0M8H0_CAEBE HDCQFSHVNSRDQCNDYTHWKDEAGKQCASKKTKDSKAMIVRSFAVLEPCALDMFTGVEFVCCPNDQTNKTADGKLSDD- 210
|H2WGW8_CAEJA HACQFSHFNSRDQCNDYQHWKEEAGKQCQAKKTKDGKPMMAKSFAVLEPCALDMFGGVEFVCCPKEQANSTKVD---EED 206
|F1KQX8_ASCSU HGCRFGHVNDRQSCNDYSHWKDEARRQCQSKVA-EGKRMSVRSFAVLEPCGLDLFTGVEFVCCPSDDKSAEHVDRVVDLD 194
|E1FYB3_LOALO HGCRFGHINDRQSCNDYAHWKDAAYKQCKTKVV-NDKRMAVRSFAVLEPCGLDLFTGVEFVCCPGDNKTEESKKKEVEED 194
|A8PZK5_BRUMA HGCRFGHINDRQSCNDYAHWKDAAYKHCKTKVV-NDKRMAVRSFAVLEPCGLDLFTGVEFVCCPGDDKTEELEKKKVEGK 217
|H3FMK4_PRIPA HDCRFNHENSQQKCNDYTSWKNEATRLCNSRKDEGGRAMIVRSFAMLEPCGLDLFTGVEYVCCPTDDADSALISKKEEDK 164
|E5SE93_TRISP KNCHFEHVDDENICKDFDYWNQTAIKNCKRRN-----SYSVLSFAMLEPCGLDMFSGVEFVCCPNRDDINADVVNVGRLS 202
              : *:* * :..: *:*:  *:: * : *  :         . ***:****.**:* ***:****
```

Figure S3. Alignment of worm APL1-D2 sequences. The Uniprot accession numbers are given on the left. Q10651_CAEEL, *Caenorhabditis. elegans*; E3LE65_CAEEL *C. remanei*, A8XKA6_CAEBR, *C. briggsae*; G0M8H0__CAEBE, *C. brenneri*; H2WGW8_CAEJA, *C. japonica*; F1KQX8_ASCSU, *Ascaris sum*; E1FYB3_LOALO, *Loa loa*; A8PZK5_BRUMA, *Brugia malayi*; H3FMK4_PRIPA, *Pristionchus pacificus*; E5SE93_TRISP, *Trichinella spiralis*. Sequences were found using Blast and aligned using Clustal as outlined in the main text. The C-terminal sequence position is given on the right. Symbols: '*' conserved residue; ':' conserved among residues of strongly similar properties; '.' conservation among residues of weakly similar properties.

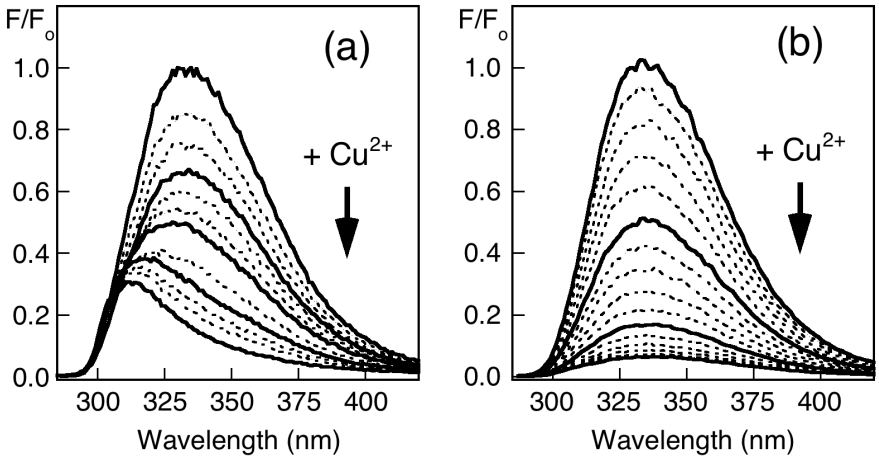

Figure S4. Change in fluorescence intensity of APL1-D2 in Mops buffer (50 mM, pH 7.3) upon titration with $CuSO_4$ (200 μM): (a) of APL1-D2 (2.0 μM); (b) of APL12-D2 (20 μM). The intensities were normalised to that at [Cu(II)] = 0 (i.e., F_0). Shown in solid lines are the spectra upon addition of 0, 1.2, 2.4, 4.0, 7.6 eqs of Cu(II) in (a) and of 0, 1, 2, 3 eqs of Cu(II) in (b).

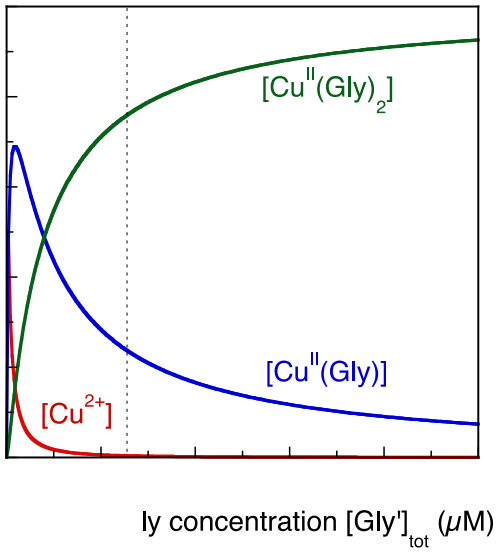

Figure S5. Speciation of $[Cu^{2+}]$, $[Cu^{II}(Gly)]$ and $[Cu^{II}(Gly)_2]$ with increasing total free glycine concentration in solution at pH 7.3.

Calculation of total free [Gly'] at $\Delta F/\Delta F_{max}$ = 0.5 for the titration curves in Figure 4b

From the titration curves in Figure 4b, when $\Delta F/\Delta F_{max} = 0.5$:

(i) half of Cu in Cu_2P (ie, 20 μM) is removed by Gly and thus total free Gly (ie, Gly that does not bind Cu) concentration

$$[Gly']_{tot} = [Gly]_{tot} - [Cu(Gly)] - 2\,[Cu(Gly)_2] \text{ and} \quad \text{(S1)}$$

$$[Cu(Gly)] + [Cu(Gly)_2] = 20\ \mu M \quad \text{(S2)}$$

(ii) $[Gly]_{tot}$ = 100 μM for P = APL1-D2 and 250 μM for P = APP-D2.

Since $[Gly']_{tot} < [Gly]_{tot}$ (eqn S1), from Cu speciation diagram in Figure S4, we may estimate that, for the titration curve (i) in Figure 4b, when $\Delta F/\Delta F_{max} = 0.5$, of total Cu that binds Gly in eqn S2, ~ 75% in $[Cu(Gly)_2]$ form and ~ 25% in $[Cu(Gly)]$ form. Thus, from eqn S1, S2:

$$[Gly']_{tot} = [Gly]_{tot} - [Cu(Gly)] - 2\,[Cu(Gly)_2]$$

$$= 100 - 0.25 \times 20 - 2 \times 0.75 \times 20$$

$$= 65\ (\mu M)$$

for the titration curve (ii) in Figure 4b, we can estimate similarly that, of total Cu that binds Gly in eqn S2, ~ 92% in $[Cu(Gly)_2]$ form and ~ 8% in $[Cu(Gly)]$ form. Thus, from eqn S1, S2:

$$[Gly']_{tot} = [Gly]_{tot} - [Cu(Gly)] - 2\,[Cu(Gly)_2]$$

$$= 250 - 0.08 \times 20 - 2 \times 0.92 \times 20$$

$$= 212\ (\mu M)$$

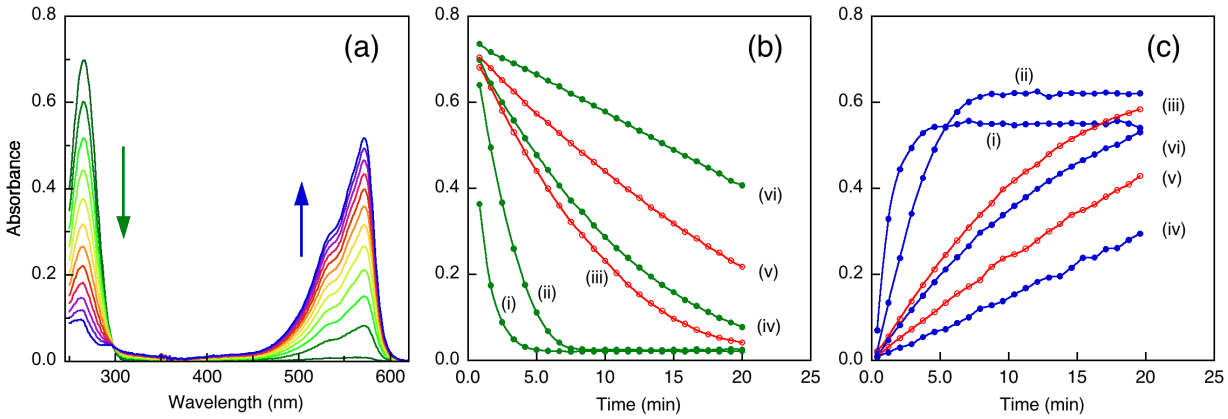

Figure S6. Catalytic aerobic oxidation of ascorbate and production of H_2O_2. (a) UV-Vis monitoring of Asc consumption and resorufin formation (thus H_2O_2 production; the spectrum of initial solution containing all components except Asc was subtracted from each recorded spectra); (b,c) kinetic curves for Asc consumption (b) and resorufin formation (c) with $[Cu]_{tot}$ = 5.0 μM plus following components as catalyst: (i) nothing; (ii) APL1-D2 (7.0 μM); (iii) APL1-D2 (7.0 μM) and Aβ16 (7.0 μM); (iv) Aβ16 (7.0 μM); (v) Aβ16 (7.0 μM) and APP-D2 (7.0 μM); (vi) APP-D2 (7.0 μM). Other initial solution conditions: [Asc] = 50 μM, [Amplex Red] ~ 45 μM; [HRP] = 0.35 U/mL. The reactions were conducted in air-saturated Mops buffer (50 mM, pH 7.4), started by introduction of catalyst and monitored by change in solution spectra.

Table S1: Summary of restraints and structural statistics for the 20 lowest energy structures of *C. elegans* APL1-D2 in aqueous solution at pH 6.9 and 30°C.

Experimental constraints		
Total	1272	
Intraresidue	402	
Sequential (|i-j| = 1)	230	
Short range (1 < |i-j| < 5)	102	
Long range (|i-j| ≥ 5)	322	
Hydrogen bonds	38	
Dihedral angles (ϕ, 51; ψ, 51)	102	
Rmsd from experimental distance restraints (Å)	0.024 ± 0.001	
Rmsd from experimental dihedral restraints (°)	0.495 ± 0.005	
Rmsd from idealized covalent geometry		
Bonds (Å)	0.004 ± 0.0001	
Angles (°)	0.542 ± 0.006	
Impropers (°)	0.350 ± 0.003	
Measures of structural quality		
E_{LJ} (kcal mol^{-1})	-280.2 ± 2.7	
Procheck percentage residues in region of Ramachandran plot		
Most favourable	76.2	
Additionally allowed	21.9	
Generously allowed	1.9	
Disallowed	0	
Angular order: residues with S(ϕ) ≥ 0.9	63	
With S(ψ) ≥ 0.9	64	
Overall G-factor	0.19 ± 0.03	
Bad contacts/ 100 residues	8.68 ± 0.89	
Violations		
Experimental distance constraints > 0.20 Å	0	
Experimental dihedral constraints > 5.0°	0	
Coordinate precision		
Mean pairwise RMSD (Å)	C^{α}, C, N,O	All heavy atoms
Residues 1-65	0.29 ± 0.12	0.85 ± 0.12